

# Improved current and charge amplifiers for driving piezoelectric loads

Andrew J. Fleming and S. O. Reza Moheimani

The School of Electrical Engineering and Computer Science, The University of Newcastle,  
Callaghan 2308, Australia.

## ABSTRACT

Piezoelectric transducers are known to exhibit less hysteresis when driven with current or charge rather than voltage. Despite this advantage, such methods have found little practical application due to the poor low frequency response of present current and charge driver designs. This paper introduces the *compliance feedback current driver* containing a secondary voltage feedback loop to prevent DC charging of capacitive loads and to compensate for any voltage or current offsets in the driver circuit. Low frequency bandwidths in the milli-Hertz range can be achieved.

**Keywords:** Current, Charge, Piezoelectric, Capacitive, Load, Amplifier, Zero Offset, Compliance, Feedback

## 1. INTRODUCTION

Piezoelectric transducers have found countless applications in such fields as vibration control<sup>1</sup>, nano-positioning<sup>2</sup>, acoustics<sup>3</sup>, and sonar<sup>4</sup>. The piezoelectric effect<sup>5,6,7</sup>, is a phenomena exhibited by certain materials where an applied electric field produces a corresponding strain and *vice versa*. The effect can be exploited in one, two, or three dimensions, for actuating, sensing, or sensori-actuating<sup>8</sup>. One common theme across the diverse literature involving piezoelectric applications is the problem of hysteresis<sup>5,7</sup>. When used in an actuating role, i.e., when current is flowing through the piezoelectric capacitance, piezoelectric transducers display a significant amount of hysteresis in the function between applied voltage and displacement<sup>5,7</sup>.

As discussed in<sup>9</sup> and references therein, a great number of techniques have been developed with the intention of reducing hysteresis. Included are displacement feedback techniques, mathematical Preisach modeling<sup>10</sup> and inversion, phase control, polynomial approximation, and current or charge actuation.

Almost all contributions in this area make reference to the well known advantages of driving piezoelectric transducers with current or charge rather than voltage<sup>11</sup>. Simply by regulating the current or charge, a five-fold reduction in the hysteresis can be achieved<sup>12</sup>. A quote from a recent paper<sup>13</sup> is typical of the sentiment towards this technique:

“While hysteresis in a piezoelectric actuator is reduced if the charge is regulated instead of the voltage<sup>11</sup>, the implementation complexity of this technique prevents a wide acceptance<sup>14</sup>”.

Although the circuit topology of a charge or current amplifier is much the same as a simple voltage feedback amplifier, due to the uncontrolled nature of the output voltage, circuit offsets generally result in the load capacitor being charged up. When the output or compliance voltage reaches the power supply rails, the output becomes saturated and distorted. The stated *complexity* invariably refers to additional circuitry required to avoid charging of the capacitor. A popular technique<sup>15,16</sup>, is to simply short circuit the load every 400 *ms* or so, thus periodically discharging the load capacitance and returning the DC compliance voltage to ground. This introduces undesirable high frequency disturbance and severely distorts low frequency charge signals.

This paper introduces a new type of current and charge amplifier capable of providing high accuracy, ultra-low frequency regulation of current or charge. The *compliance feedback current or charge amplifier* contains an additional output voltage feedback loop (resulting in only a single additional opamp) to effectively estimate and reject all sources of DC offset. This technique is intended as a viable alternative for previously presented current and charge amplifiers. A full analysis is provided to clarify the problem and to illustrate the simplicity of the solution.

---

(Send correspondence to [andrew@ee.newcastle.edu.au](mailto:andrew@ee.newcastle.edu.au))

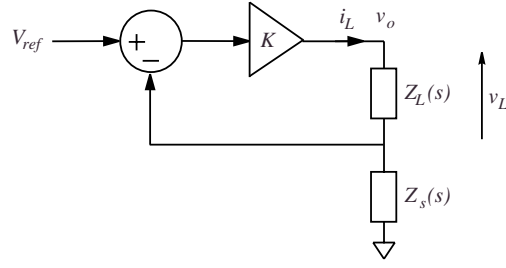


Figure 1. Generic current source.

## 2. COMPLIANCE FEEDBACK CURRENT / CHARGE DRIVERS.

Consider the simplified diagram of a generic current source<sup>17</sup> shown in Figure 1. The high gain feedback loop and voltage driver works to equate the applied reference voltage  $v_{ref}$ , to the sensing voltage  $v_s$ . In the Laplace domain, at frequencies well within the bandwidth of the control loop, the load current  $I_L(s)$  is equal to  $V_{ref}(s)/Z_s(s)$ .

If  $Z_s(s)$  is a resistor  $R_s$ ,

$$I_L(s) = V_{ref}(s)/R_s. \quad (1)$$

i.e., we have a current amplifier with gain  $1/R_s$  A/V.

If  $Z_s(s)$  is a capacitor  $C_s$ ,

$$\dot{q}_L = I_L(s) = V_{ref}(s)C_s s, \quad (2)$$

$$q_L = V_{ref}(s)C_s. \quad (3)$$

i.e., we have a charge amplifier with gain  $C_s$  Columbs/V.

As mentioned in the introduction, the foremost difficulty in employing such devices to drive highly capacitive loads is that of DC current or charge offsets. Inevitably, the voltage measured across the sensing impedance will contain a non-zero voltage offset, this and other sources of voltage or current offset in the circuit will result in a net output offset current or charge. As a capacitor integrates DC current, the uncontrolled output voltage will tend towards infinity and saturate at the power supply rails. Any offset in  $v_o$  limits the compliance range of the current source and will eventually cause saturation. To limit the DC impedance of the load, i.e., limiting the DC compliance offset for a certain output offset current, a parallel resistance is often used. With  $Z_L(s) = \frac{1}{C_L s} || R_L$ , the actual current  $I_{Lc}(s)$  flowing through the load capacitor is now,

$$I_{Lc}(s) = I_L(s) \frac{s}{s + \frac{1}{R_L C_L}}. \quad (4)$$

Additional dynamics have been added to the current source, the transfer function now contains a high-pass filter with cutoff  $\omega_c = \frac{1}{R_L C_L}$ . That is,

$$\frac{I_{Lc}(s)}{V_{ref}(s)} = \frac{1}{R_s} \frac{s}{s + \frac{1}{R_L C_L}}. \quad (5)$$

In contrast to the infinite DC impedance of a purely capacitive load, the load impedance now flattens out towards DC at  $\omega_c = \frac{1}{R_L C_L}$ , and has a DC impedance of  $R_L$ . Thus, a DC offset current of  $i_{dc}$  results in a compliance offset of  $v_{dc} = i_{dc} R_L$ . In a typical piezoelectric driving scenario, with  $C_L = 100$  nF, and  $i_{dc} = 1$   $\mu$ A, a 1 M $\Omega$  parallel resistance is required to limit the DC compliance offset to 1 V. The frequency response from an applied reference voltage to the actual capacitive load current  $I_{Lc}(s)$  is shown in Figure 2. Phase lead exceeds 5 degrees below 18 Hz. Such poor low frequency response precludes the use of current amplifiers in applications requiring accurate

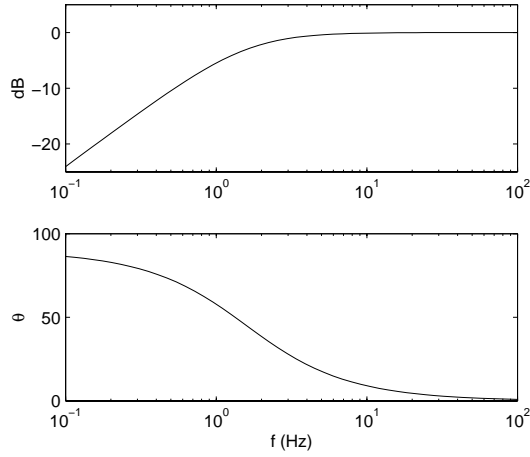


**Figure 2.** Typical frequency response from an applied reference voltage to the actual capacitive load current  $I_{Lc}(s)$ .

low frequency tracking, e.g., Atomic Force Microscopy<sup>2</sup>. The advantages of piezoelectric current excitation are lost to the practical electronic difficulties in constructing a current source.

The following section introduces a new type of current source. The *compliance feedback current amplifier* compensates for DC compliance offset without the addition of a parallel resistance. Low frequency bandwidths in the milli-Hertz range can be achieved with basic components.

## 2.1. Analysis of compliance feedback current and charge amplifiers.

The aim of this section is to introduce a generalized compliance feedback current or charge amplifier. From the general description of its operation, we introduce a class of controllers that achieve excellent ultra-low frequency tracking, and complete rejection of DC compliance offset.

Figure 3 shows the schematic diagram of a compliance feedback current source. Neglecting the input associated with the compliance controller  $C(s)$ , the circuit is simply a realization of the simplified diagram in Figure 1. The inverted\* reference voltage  $v_{ref}$ , is maintained (by the high gain feedback loop) across the sensing impedance  $Z_s(s)$ . Thus,  $I_L(s) = -V_{ref}(s)/Z_s(s)$ . In this implementation the voltage driver contains three stages<sup>17</sup>, the differential input, the transconductance stage, and the current amplifier. Simply,  $v_o = K(v_+ - v_-)$ , where  $K$  is the combined gain of the differential and transconductance stage.

For high power, or ultra-efficient current and charge amplifiers, the output driver stage can be replaced with a pulse width modulated DC-AC inverter<sup>18,19</sup>. The time delay inherent in switching amplifiers, now enclosed in the current or charge feedback loop will limit the high frequency bandwidth of the amplifier. Apart from the addition of switching noise and current ripple, all of the following results for linear amplifiers apply.

The voltages and currents of interest are related in the system block diagram shown in Figure 4. The auxiliary signal  $v_p$  models a load internal voltage source. For example, the piezoelectric voltage internal to a piezoelectric transducer. By definition, the polarity of the source hinders the current  $i_L$ .

To control the amplifier, there are two objectives. The first is to ensure good reference current or charge tracking performance. The second is to provide low frequency and DC regulation of the compliance voltage  $v_o$ . Obviously we cannot achieve both goals independently. To understand the trade-off between tracking performance and compliance regulation, we will study two transfer functions, the transfer function from an applied reference voltage  $V_{ref}(s)$  to the voltage measured across the sensing impedance  $V_s(s)$ , and the transfer function from an applied reference voltage  $V_{ref}(s)$  to the compliance voltage  $V_o(s)$ .

---

\*The inversion of  $v_{ref}$  is performed purely for convenience when implementing shunt damping circuits. For this application, the current is usually defined flowing *into* the current source.

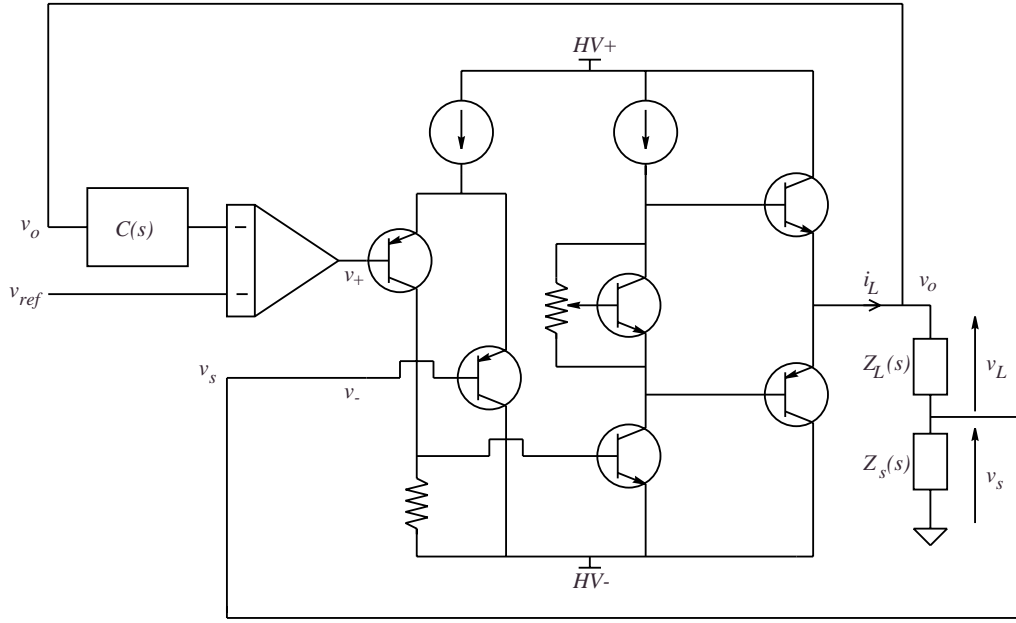


**Figure 3.** Simplified schematic of a compliance feedback current amplifier.

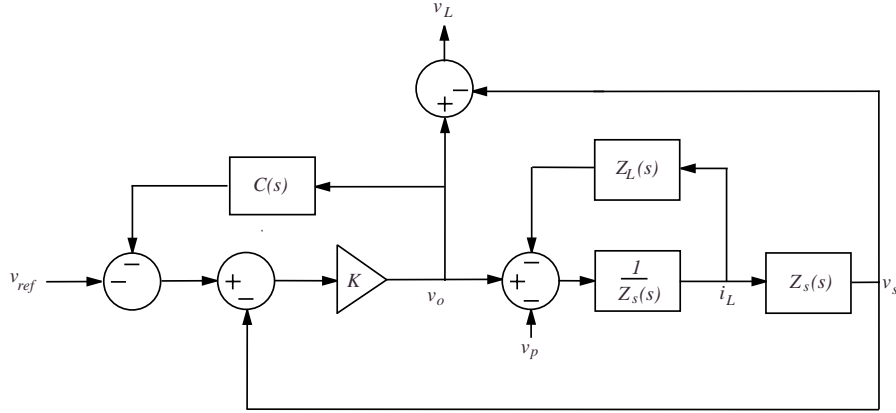


**Figure 4.** System block diagram of the circuit shown in Figure 3.

For a current source connected to a capacitive load,  $Z_s(s) = R_s$  and  $Z_L(s) = \frac{1}{C_L s}$ , assuming  $V_p(s) = 0$ ,

$$\frac{V_s(s)}{V_{ref}(s)} = \frac{-KR_s C_L s}{(1 + KC(s))(R_s C_L s + 1) + KR_s C_L s} \quad (6)$$

$$\frac{V_o(s)}{V_{ref}(s)} = \frac{-KR_s C_L s - K}{(1 + KC(s))(R_s C_L s + 1) + KR_s C_L s} \quad (7)$$

The effect of three compliance controllers is discussed below. Figures 5, 6, and 7 compare the responses of each control strategy, proportional, integral, and PI. To be fair, numerical values are selected so that each strategy has a comparable low frequency tracking performance.

(a) Our first choice of controller is simply a proportional controller  $C(s) = c$ . The effect on the transfer functions  $\frac{V_s(s)}{V_{ref}(s)}$  and  $\frac{V_o(s)}{V_{ref}(s)}$  is shown in Figures 5 (a), and 6 (a). The transient response of the compliance

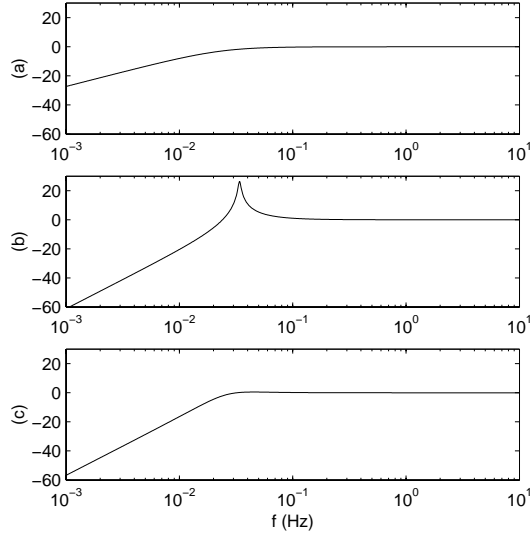


**Figure 5.** The current tracking performance  $\frac{V_s(s)}{V_{ref}(s)}$  of a current source with capacitive load and compliance controller (a) Proportional (b) Integral (c) PI.

voltage to a step in DC offset current is shown in Figure 7 (a). Analogous to the effect of adding a parallel resistor, the transfer function  $\frac{V_o(s)}{V_{ref}(s)}$  *flattens out* towards DC limiting the integration of offset currents. As shown in Figure 7 (a), any offset current results in a large compliance offset. The benefit is that the voltage across the sensing resistance is still proportional to the load current, i.e., even though the dynamic response is no better than a simple resistor, we are now able to measure load current even outside the bandwidth of the amplifier.

(b) To eliminate DC compliance offset, the next obvious choice is integral control  $C(s) = \frac{\alpha}{s}$ . Referring to figures 5, 6, and 7 (b), the DC compliance offset is completely rejected but we have introduced a lightly damped low frequency resonance. As demonstrated in Figure 7 (b), the result is an extremely poor settling time in the transient response.

(c) Proportional-integral (PI) control  $C(s) = \frac{\alpha s + \delta}{s}$  achieves complete rejection of offset currents while exhibiting a fast settling time in the transient compliance response. Using the variables  $\alpha$ ,  $\delta$ , and  $R_s$ , an arbitrary low frequency bandwidth can be obtained with full control over the system damping. Figures 5, 6, and 7 (c), show a superior performance in all of the qualifying responses. A PI controller is easily implemented using the simple opamp circuit shown in Figure 8. The corresponding transfer function is,

$$\frac{V_{out}(s)}{V_{in}(s)} = \frac{\frac{1}{C_2 R_1} + \frac{R_2}{R_1} s}{s} \quad (8)$$

For a charge amplifier connected to a capacitive load,  $Z_s(s) = \frac{1}{C_s s}$  and  $Z_L(s) = \frac{1}{C_L s}$ , we may write,

$$\frac{V_s(s)}{V_{ref}(s)} = \frac{-K C_L}{(1 + K C(s))(C_L + C_s) + K C_L} \quad (9)$$

$$\frac{V_o(s)}{V_{ref}(s)} = \frac{-K C_L - K C_s}{(1 + K C(s))(C_L + C_s) + K C_L} \quad (10)$$

The compliance controller design for charge amplifiers is considerably easier. Simple integral control ( $C(s) = \frac{\alpha}{s}$ ) results in a first order response with complete regulation of DC offsets.

$$\frac{V_o(s)}{V_{ref}(s)} = \frac{-K C_L s - K C_s}{(K C_L + C_L + C_s)s + K \alpha (C_L + C_s)} \quad (11)$$

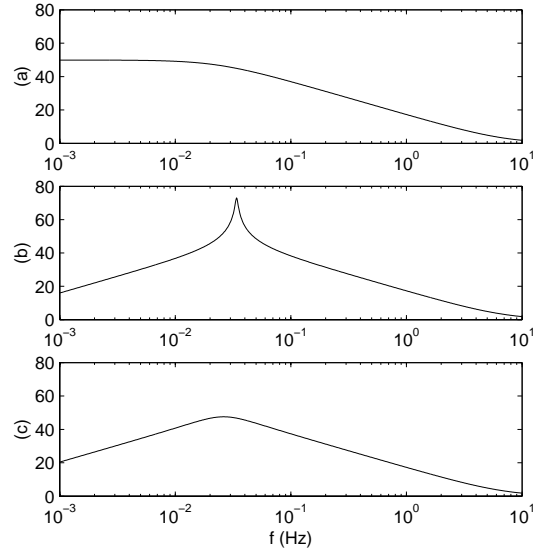


**Figure 6.** The compliance regulation performance  $\frac{V_o(s)}{V_{ref}(s)}$  of a current source with capacitive load and compliance controller (a) Proportional (b) Integral (c) PI.

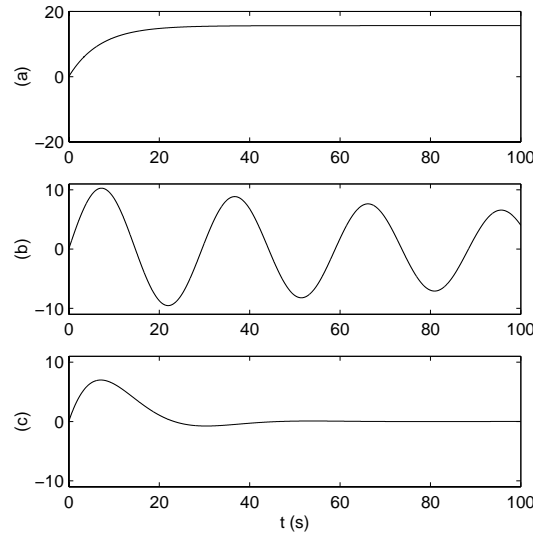


**Figure 7.** The transient response of the compliance voltage  $V_s(s)$  to a step in DC offset current. (a) Proportional (b) Integral (c) PI.

The location of the closed loop pole is easily manipulated by the variable  $\alpha$ .

## 2.2. Experimental Results

In this section, experimental results are presented for a prototype current and charge amplifier shown in Figure 9.

To illustrate the operation of the current amplifier, a  $1 \mu F$  capacitor is driven at low frequencies with a current sensing resistor of  $220 k\Omega$ . With  $C(s) = \frac{0.004s+0.00016}{s}$ , the simulated compliance and tracking frequency responses are shown in Figures 10 and 11. The transient response to a step change in current offset is shown in Figure 13. A  $100 mHz$  signal is applied to examine the low frequency tracking performance, the reference and measured currents are shown in Figure 12.

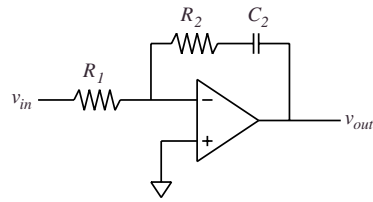


**Figure 8.** Opamp implementation of an inverting PI controller.



**Figure 9.** Photograph of a prototype current / charge amplifier.

Similar experiments were carried out for a charge amplifier. Using a sensor capacitance of  $10 \mu F$ , the compliance controller  $C(s) = \frac{0.001}{s}$  provides the desired response. Analogous frequency and time domain results are presented in Figures 14, 15, 16, and 17.

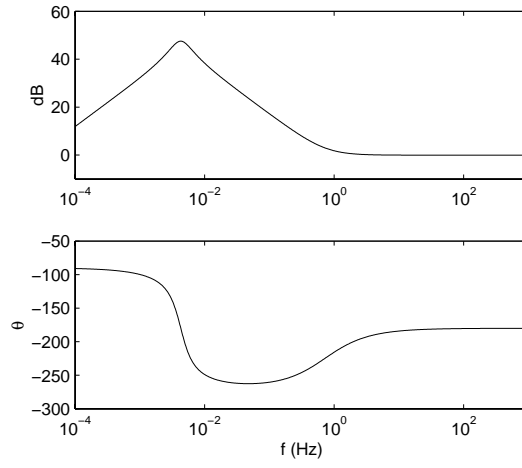


**Figure 10.** Simulated compliance frequency response  $\frac{V_o(s)}{V_{ref}(s)}$  of the prototype current source.

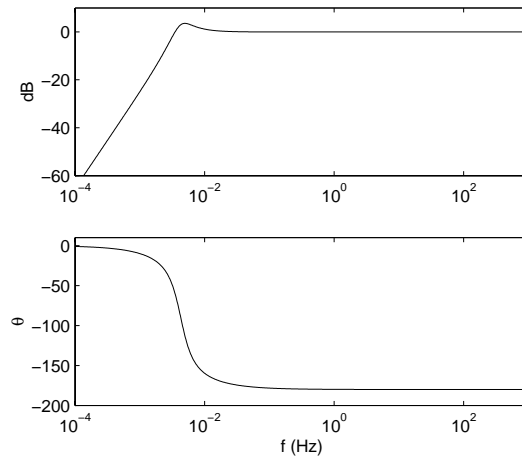


**Figure 11.** Simulated tracking frequency response  $\frac{V_s(s)}{V_{ref}(s)}$  of the prototype current source.

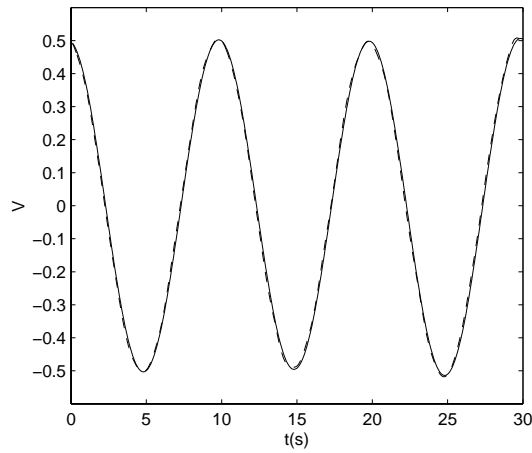


**Figure 12.** Reference (—) and measured current (- -).

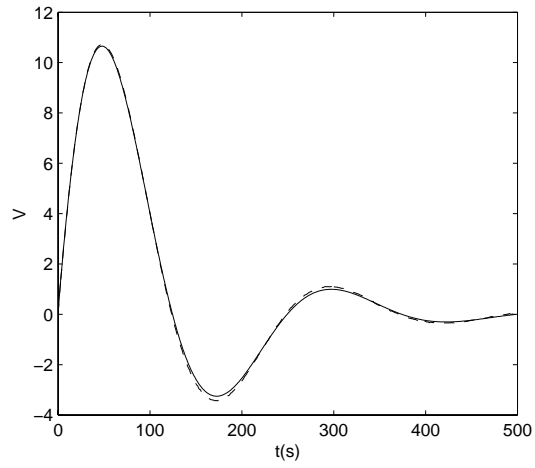


**Figure 13.** Simulated (—) and measured (---) compliance response to a step change in current offset.

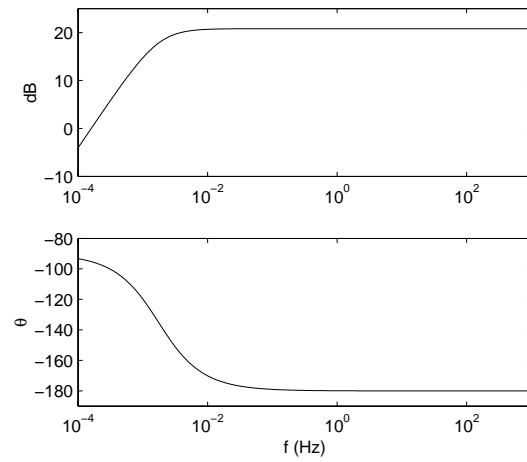


**Figure 14.** Simulated compliance frequency response  $\frac{V_o(s)}{V_{ref}(s)}$  of the prototype charge amplifier.

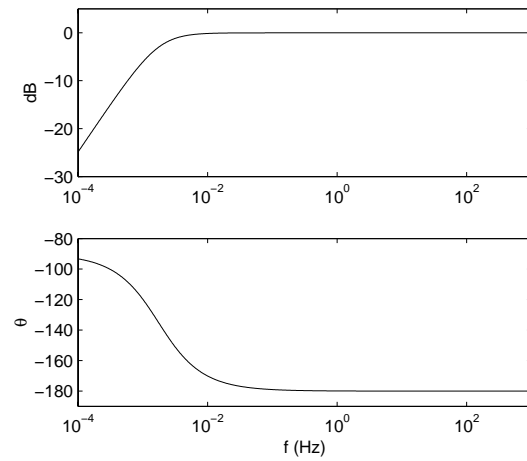


**Figure 15.** Simulated tracking response  $\frac{V_s(s)}{V_{ref}(s)}$  of the prototype charge amplifier.

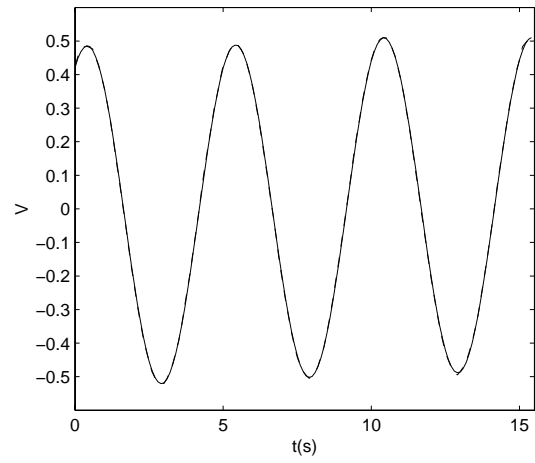


**Figure 16.** Reference (—) and measured charge (- -).

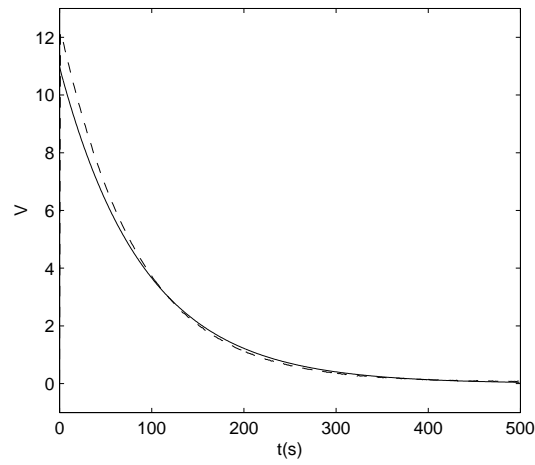


**Figure 17.** Simulated (—) and measured (- -) compliance response to a step change in current offset.

### 3. CONCLUSIONS

A new type of current and charge amplifier has been introduced. By feeding back the amplifier's compliance voltage, the effect of DC circuit offsets can be eliminated. Experimental results show excellent low frequency current and charge tracking and complete rejection of DC offsets.

A prototype compliance feedback amplifier connected to a purely capacitive load is shown to accurately realize low frequency current and charge signals of 100 and 200 *mHz* respectively.

**Acknowledgement.** This research was supported in part by the Australian Research Council under Discovery grant DP0209396, and in part by the University of Newcastle RMC project grant.

### REFERENCES

1. N. W. Hagood, W. H. Chung, and A. v. Flowtow, "Modelling of piezoelectric actuator dynamics for active structural control," *Journal of Intelligent Material Systems and Structures* **1**, pp. 327–354, 1990.
2. D. Croft, G. Shedd, , and S. Devasia, "Creep, hysteresis and vibration compensation for piezoactuators: Atomic force microscopy application," in *Proc. American Control Conference*, pp. 2123–2128, (Chicago, Illinois), June 2000.
3. C. Niezrecki and H. H. Cudney, "Feasibility to control launch vehicle internal acoustics using piezoelectric actuators," *Journal of Intelligent Material Systems and Structures* **12**, pp. 647–660, September 2001.
4. D. Stansfield, *Underwater Electroacoustic Transducers*, Bath University Press and Institute of Acoustics, Bath, UK, 1991.
5. H. J. M. T. A. Adriaens, W. L. d. Koning, and R. Banning, "Modeling piezoelectric actuators," *IEEE/ASME transactions on mechatronics* **5**, pp. 331–341, December 2000.
6. *IEEE Standard on Piezoelectricity*, ANSI/IEEE standard 176-1987, 1987.
7. B. Jaffe, W. R. Cook, and H. Jaffe, *Piezoelectric Ceramics*, Academic Press, 1971.
8. J. J. Dosch, D. J. Inman, and E. Garcia, "A self-sensing piezoelectric actuator for collocated control," *Journal of Intelligent Material Systems and Structures* **3**, pp. 166–185, January 1992.
9. K. Furutani, M. Urushibata, and N. Mohri, "Improvement of control method for piezoelectric actuator by combining charge feedback with inverse transfer function compensation.," in *Proc. IEEE International Conference on Robotics and Automation*, pp. 1504–1509, (Leuven, Belgium), May 1998.
10. I. D. Mayergoyz, *Mathematical Models of Hysteresis*, Springer Verlag, New York, 1991.
11. C. V. Newcomb and I. Flinn, "Improving the linearity of piezoelectric ceramic actuators," *IEE Electronics Letters* **18**, pp. 442–443, May 1982.
12. P. Ge and M. Jouaneh, "Tracking control of a piezoelectric actuator," *IEEE Transactions on control systems technology* **4**, pp. 209–216, May 1996.
13. J. M. Cruz-Hernandez and V. Hayward, "Phase control approach to hysteresis reduction," *IEEE transactions on control systems technology* **9**, pp. 17–26, January 2001.
14. H. Kaizuka and B. Siu, "Simple way to reduce hysteresis and creep when using piezoelectric actuators.," *Japan Journal of Applied Physics, part 2 - Letters* **27**, pp. 773–776, May 1988.
15. A. M. J, E. Garcia, and D. V. Newton, "Precision position control of piezoelectric actuators using charge feedback," *Journal of Guidance, control, and dynamics* **18**, pp. 1068–1073, September-October 1995.
16. R. Comstock, "Charge control of piezoelectric actuators to reduce hysteresis effects," *United States Patent 4,263,527, Assignee: Charles Stark Draper Lab* , 1981.
17. P. Horowitz and W. Hill, *The Art of Electronics*, Cambridge University Press, 1980.
18. S. Chandrasekaran, D. K. Lindner, and R. C. Smith, "Optimized design of switching amplifiers for piezoelectric actuators," *Journal of Intelligent Material Systems and Structures* **11**, pp. 887–901, November 2000.
19. N. Mohan, T. M. Undeland, and W. P. Robbins, *Power Electronics: Converters, Applications, and Design*, Wiley, New York, 1995.